



Universiteit
Leiden
The Netherlands

Depairing current behavior in superconducting Nb/Pd₈₁Ni₁₉ bilayers

Cirillo, C.; Rusanov, A.Yu.; Bell, C.; Aarts, J.

Citation

Cirillo, C., Rusanov, A. Y., Bell, C., & Aarts, J. (2007). Depairing current behavior in superconducting Nb/Pd₈₁Ni₁₉ bilayers. *Physical Review B*, 75(17), 174510.
doi:10.1103/PhysRevB.75.174510

Version: Not Applicable (or Unknown)

License: [Leiden University Non-exclusive license](#)

Downloaded from: <https://hdl.handle.net/1887/45199>

Note: To cite this publication please use the final published version (if applicable).

Depairing current behavior in superconducting Nb/Pd₈₁Ni₁₉ bilayers

C. Cirillo,* A. Rusanov,[†] C. Bell, and J. Aarts

Kamerlingh Onnes Laboratory, Leiden University, P.O. Box 9504, 2300 RA Leiden, The Netherlands

(Received 26 November 2006; published 15 May 2007)

We have investigated superconductor/ferromagnetic bilayers consisting of Nb/Pd₈₁Ni₁₉ with varying thickness of the ferromagnet (F) layer d_F in order to compare the behavior of the superconducting transition temperature T_c with that of the depairing current density J_{dp} . For $T_c(d_F)$, we find the usual behavior, with a minimum around $d_F=3$ nm, which signifies the transition to an oscillatory order parameter in the F layer. For J_{dp} , which was measured down to $T/T_c \approx 0.5$ using a pulsed-current technique, we find that the behavior can be well described by the Kupriyanov-Lukichev (KL) theory (Fiz. Nizk. Temp. **6**, 445 (1980) [Sov. J. Low Temp. Phys. **6**, 210 (1980)]), and therefore also by $J_{dp} \propto (1 - T/T_c)^{3/2}$ in the Ginzburg-Landau (GL) regime close to T_c . Extrapolating the GL regime to $T=0$ yields $J_{dp}^{GL}(0)$, which, as a function of d_F , behaves similarly to $T_c(d_F)$ with a shallow minimum around $d_F=3-4$ nm. At some temperature below T_c , most samples break away from the KL curve to higher values of J_{dp} , indicating a current-induced breakdown of the inhomogeneous state. Moreover, we find a significantly increased width of the transition to the normal state in the regime of the oscillatory order parameter.

DOI: 10.1103/PhysRevB.75.174510

PACS number(s): 74.25.Sv, 74.45.+c, 74.78.-w

I. INTRODUCTION

Proximity effects between superconductor/ferromagnet (S/F) hybrids constitute a very active field of research, due both to the rich physics originating from the coexistence of the two competing ordered phases and to the numerous suggestions for the engineering applications for these heterostructures.¹ In these systems, superconductivity is suppressed in the superconductor over the coherence length ξ_S , but it is induced in the ferromagnet in a nontrivial way. The presence of the exchange field E_{ex} in F causes an energy shift between the quasiparticles of the pair entering the ferromagnet, and this results in the creation of Cooper pairs with nonzero momentum.² This implies that the superconducting order parameter, Ψ , does not simply decay in the ferromagnetic metal, as it would happen in a normal one, but also oscillates along the direction perpendicular to the interface. In the dirty limit, and for the case that $E_{ex} \gg k_B T$ (with T the temperature), the behavior can be described by $\Psi \propto \exp(-x/\xi_F) \cos(x/\xi_F)$, where x is the coordinate into the F layer. In this approximation, $\xi_F = \sqrt{\hbar D_F / E_{ex}}$ measures both the decay length and the oscillation wavelength of the order parameter, and is often called the coherence length in the F metal. The oscillation period is then given by $\lambda_F = 2\pi\xi_F$. The inhomogeneous character of the superconducting order parameter, which may be interpreted as a manifestation of a so-called Larkin-Ovchinnikov-Fulde-Ferrell (LOFF)^[3,4] phase, reveals itself in a nonmonotonic behavior of all the parameters depending on the Ψ . Signatures of this inhomogeneous state are the well-known nonmonotonic dependence of the transition temperature T_c on the ferromagnetic layer thickness d_F (for a review, see, for instance, Ref. 5) and the negative critical current in $S/F/S$ Josephson junctions⁶⁻⁸ (π junction) or the reversed density of states in $S/F/I/N$ (I an insulator, N a normal metal) tunnel junctions.⁹

One of the drawbacks of standard resistive measurements is that no information is obtained below T_c , which would be of interest since T_c is usually quite sensitive to sample preparation issues and also, e.g., for investigating superconducting spin valves of type $F_1/S/F_2$. In such systems, varying the

relative directions of the magnetization of the two F layers leads to different values for T_c , as argued theoretically,¹⁰⁻¹² but the observed effects are generally small.¹³⁻¹⁵ A quantity sensitive to order parameter changes below T_c is the depairing current density J_{dp} . A simple advantage of J_{dp} over T_c is that, where T_c probes the maximum value of the superconducting order parameter in the sample, J_{dp} comes from an average over the layer thickness, which also involves lower values of Ψ .¹⁶ The aims of this work are to probe the inhomogeneous character of the superconducting order parameter in bilayers of Nb and Pd₈₁Ni₁₉ and to directly compare the information from T_c and J_{dp} upon varying the PdNi layer thickness d_{PdNi} . The paper is organized as follows. We first describe the magnetic characterization of the PdNi layers. Next we present data on $T_c(d_{PdNi})$ for constant thickness of the Nb layer as well as data on $T_c(d_{Nb})$ for constant thickness of the PdNi layer. Both data sets are used to give a consistent description of the proximity effect using the model developed by Fominov *et al.*¹⁷ This yields the microscopic proximity effect parameters, in particular, estimates of the wavelength λ_F of the order parameter oscillation in the PdNi layer and the interface transparency parameter γ_b . Then we present the data on the current (I)-voltage (V) characteristics and the ensuing $J_{dp}(d_{PdNi})$ and we discuss how to analyze them, guided by the theory of Kupriyanov and Lukichev (KL).¹⁸ In the Ginzburg-Landau regime, we find good agreement between the two types of measurements, but we also find deviations from KL behavior which indicate a breakdown of the suppression of the order parameter by the F layer at lower temperatures and/or higher current densities. Moreover, the width of the transition in $V(I)$ to the normal state appears significantly enhanced above $d_F = \lambda_F/4$, in the regime of the oscillatory order parameter.

II. EXPERIMENTAL DETAILS

Si/Nb/Pd_{1-x}Ni_x bilayers were grown on Si(100) substrates in a UHV dc diode magnetron sputtering system with a base pressure less than 10^{-9} mbar and sputtering argon

pressure of 4×10^{-3} mbar. The Nb and $\text{Pd}_{0.81}\text{Ni}_{0.19}$ layers were deposited at typical rates of 0.1 and 0.2 nm/s, respectively, measured by a quartz crystal monitor calibrated by low-angle x-ray reflectivity measurements. A $\text{Pd}_{1-x}\text{Ni}_x$ target with $x=0.10$ was used. This stoichiometry was not conserved in the samples as revealed by Rutherford-backscattering analysis, which gives a Ni concentration of $x=0.19$. Two different sets of bilayers were prepared. In order to study the T_c dependence as a function of the ferromagnetic layer thickness, d_{PdNi} , samples were deposited with constant Nb thickness ($d_{\text{Nb}}=14$ nm) and variable thickness of the $\text{Pd}_{0.81}\text{Ni}_{0.19}$ layers. This set is named F. The behavior of $T_c(d_{\text{Nb}})$ was investigated on another set of bilayers (set S) consisting of a $\text{Pd}_{0.81}\text{Ni}_{0.19}$ layer with constant thickness ($d_{\text{PdNi}}=19$ nm) and a Nb layer with variable thickness ($d_{\text{Nb}}=10\text{--}150$ nm). Moreover, one set of Nb single films was deposited ($d_{\text{Nb}}=14\text{--}200$ nm) in order to study the thickness dependence of both the critical temperature and the electrical resistance. Samples of $\text{Pd}_{0.81}\text{Ni}_{0.19}$ with different thicknesses were also fabricated to study the electrical and magnetic properties of the alloy.¹⁹ The critical temperatures were resistively measured using a standard dc four-probe technique with a commercial Quantum Design physical property measurement system. T_c was defined as the midpoint of the transition curve. The depairing current measurements were performed on the samples of set F in a dedicated ^4He cryostat equipped with a Permalloy screen to minimize the effects of unwanted external magnetic fields. In this kind of measurements, great care must be taken to assure a uniform current distribution over the width of the strip²⁰ and to avoid Joule heating of the samples.²¹ The first issue requires samples with a bridge width w comparable with the penetration depth λ and the coherence length ξ of the superconductor, respectively. Recent results^{16,22} on Nb and MoGe single films and Fe/Nb/Fe trilayers, however, give us reason to expect uniform current distributions for $w \approx 1.5 \mu\text{m}$. A classical pseudo-4-point geometry (meaning two contacts, each used for a current and a voltage lead) was defined using e-beam lithography. The structuring process, consisting of two main stages (e-beam writing and argon-ion etching), provided sharp-edged bridges. Figure 1 shows an image of a typical sample (bridge and contacts) made by electron microscopy. Since the width of the bridges is sensitive to the treatment of the photoresist needed in the etching process, the width of each bridge was checked individually by electron microscopy in order to have a correct value for the determination of the current density. Values were found in the range of $1.5\text{--}2.1 \mu\text{m}$. To avoid sample heating, the $V(I)$ characteristics were measured with a pulsed technique. A Keithley 220 current source provided short current pulses ($t_{\text{pulse}}=3\text{--}5$ ms) with growing amplitude, which were followed by a long pause ($t_{\text{pause}}=7$ s). To provide a good thermal exchange, the samples were glued with silver paint on the massive brass sample holder of the insert, in a helium gas pressure of about 10^2 mbar. With this method, already successfully applied to measure $J_{dp}(T)$ dependence in Nb and amorphous MoGe thin films,²² test measurements were performed on a single Nb film. The results reconfirmed that $J_{dp}(T)$ behaves according to KL theory and allowed the esti-

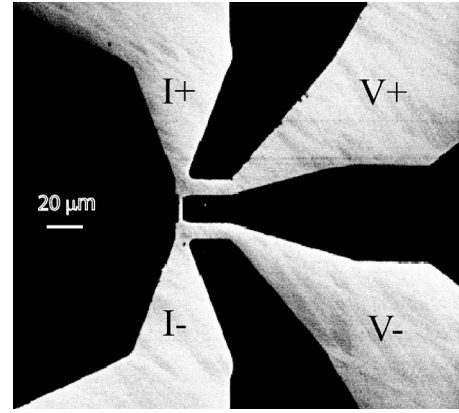


FIG. 1. Electron microscopy image of a structured Nb/PdNi bilayer sample for depairing current measurements. The bridge is $1.5 \mu\text{m}$ wide and $15 \mu\text{m}$ long. The contacts for current (I) and voltage (V) are indicated.

mate of the zero-temperature critical current density $J_{dp}^{\text{Nb}}(0) \approx 9 \times 10^{11} \text{ A/m}^2$.

III. MAGNETIC PROPERTIES

Magnetic characterization was performed on a number of $\text{Pd}_{0.81}\text{Ni}_{0.19}$ single films using a commercial Quantum Design superconducting quantum interference device magnetometer (MPMS-5S). In all the reported measurements, the field was applied parallel to the sample surface. Figure 2 shows the hysteresis loop of an unstructured film 19.2 nm thick, whose dimensions and density are $0.8 \times 0.55 \text{ cm}^2$ and 11.41 g/cm^3 , respectively. At $T=10 \text{ K}$, the saturation magnetization is $M_{\text{sat}}=0.35 \mu_B/\text{atom}$. At a temperature $T=5 \text{ K}$, M_{sat} varies between $M_{\text{sat}}=0.27$ and $0.35 \mu_B/\text{atom}$ for all the samples in the thickness range from 3.3 to 70 nm . The Curie temperature was also determined for a wide set of samples from

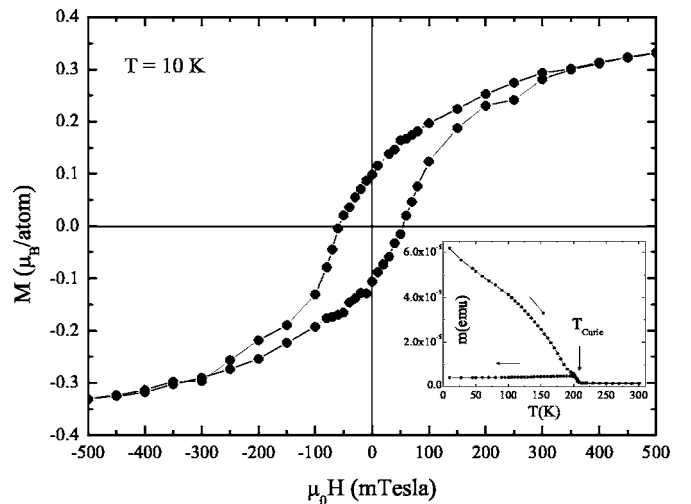


FIG. 2. Magnetization loop for a single $\text{Pd}_{0.81}\text{Ni}_{0.19}$ film, 19.2 nm thick, at $T=10 \text{ K}$. Inset: Remanent magnetic moment m as a function of the temperature T for the same sample, after saturation at $T=5 \text{ K}$; arrows show the direction of the temperature change.

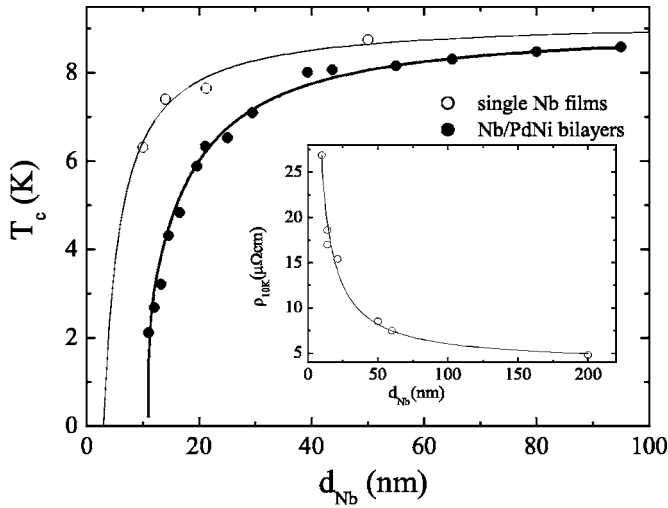


FIG. 3. Critical temperature T_c versus Nb thickness d_{Nb} in Nb/Pd_{0.86}Ni_{0.19} bilayers of series S ($d_{\text{PdNi}}=19$ nm). The thick line is the result of the theoretical calculations in the single-mode approximation. The fitting parameters are given in the text. Open symbols refers to single Nb films. The light line describes the phenomenological T_c thickness dependence of Nb single films. Inset: thickness dependence of the low-temperature resistivity as a function of the single Nb thickness. The line is a guide for the eyes.

$m(T)$ measurements. The films were magnetized to saturation at 5 K, the field was then removed, and $m(T)$ was measured up to 300 K and down again to 5 K. T_{Curie} was defined as the point where irreversibility appears when cooling down the sample. Typical $m(T)$ behavior is reported in the inset of Fig. 2 for the same film. The Curie temperature can be estimated to be $T_{\text{Curie}} \approx 210$ K, in agreement with the values reported for bulk samples at this concentration.^{23,24} The $m(T)$ measurements, performed on samples with different d_{PdNi} , give no indication of a thickness dependence of T_{Curie} for $d_{\text{PdNi}} = 3.3\text{--}70$ nm.¹⁹

IV. CRITICAL TEMPERATURES

Superconducting transition temperatures T_c were measured for all sample sets. Figure 3 shows the data for $T_c(d_{\text{Nb}})$ (set S), which show the standard behavior for S/F bilayers with a critical thickness for the S layer $d_{\text{cr}}^S \approx 11$ nm. Single Nb films were also investigated, and the dependence of T_c on thickness is also shown in Fig. 3. The line through the data points is obtained from the phenomenological dependence $T_c(d_{\text{Nb}}) = T_{c0}(1 - d_0/d_{\text{Nb}})$, with $T_{c0} = 9.2$ K and $d_0 = 2.9$ nm. The critical temperature is strongly reduced as the thicknesses is lowered below 20 nm. In the same thickness range, the low-temperature resistivity of the films drastically increases, as shown in the inset of Fig. 3. Measurements of the upper critical field performed earlier on similar films show that the latter effect can be connected to a decrease of the elastic electronic mean free path ℓ_e from around 8 nm at large thickness to less than 2 nm at $d_{\text{Nb}} \approx 10$ nm. We assume that this is due to smaller grain sizes at the onset of growth. The decrease of T_c , in turn, can be correlated with the increase in resistivity, which follows a universal behavior irre-

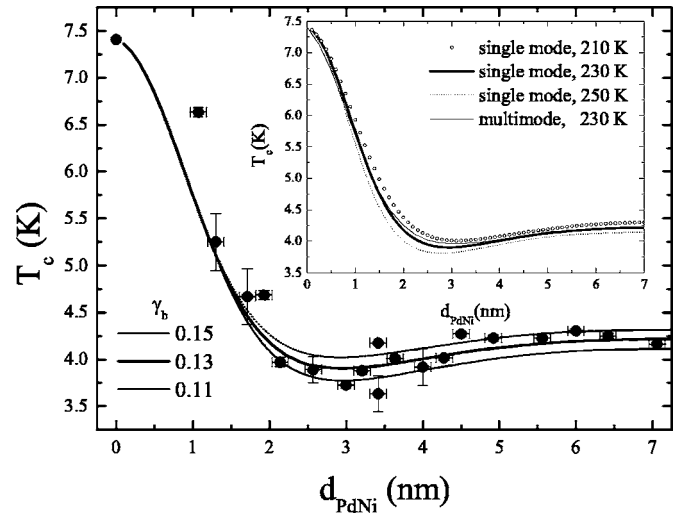


FIG. 4. Critical temperature T_c versus PdNi thickness d_{PdNi} in Nb/Pd_{0.81}Ni_{0.19} bilayers with constant Nb thickness $d_{\text{Nb}} = 14$ nm. Different lines (dotted, thick solid, and light solid) are the results of the theoretical fit in the single-mode approximation for different values of γ_b . Inset: comparison between the single-mode (thick line) and the multimode (light line) calculations for $E_{\text{ex}} = 230$ K. The dotted line and the circles are the results of single-mode calculations for $E_{\text{ex}} = 250$ K and $E_{\text{ex}} = 210$ K, respectively.

spective of the actual source of the (increased) disorder, as shown by Park and Geballe.²⁵ The data for the $T_c(d_{\text{PdNi}})$ of set F ($d_{\text{Nb}} = 14$ nm) are given in Fig. 4. The curve exhibits a rapid drop as the ferromagnetic thickness is increased until a shallow minimum is reached for $d_{\text{PdNi}} \approx 3.0\text{--}3.5$ nm. A thickness-independent saturation value is observed for d_{PdNi} above 5 nm.

The behavior of both $T_c(d_F)$ and $T_c(d_S)$ can be analyzed in the framework of the proximity effect model developed in Ref. 17 based on the linearized Usadel equation. This yields values for E_{ex} of the F layer and for the interface transparency parameter γ_b , with the dual purpose of demonstrating that these bilayers behave as expected for our materials and of extracting a value for the oscillation period λ_F in the ferromagnet. We follow the same strategy adopted for the description of Nb/Pd_{0.86}Ni_{0.14} bilayers,²⁶ but we briefly reiterate the parameters and the formulas used for these calculations in the Appendix. We start with the F series and use the following input parameters to model $T_c(d_F)$. For $d_F = 0$, we use $T_{cS} = 7.41$ K, interpolated from the behavior of the single Nb films at 14 nm. From $\rho_{\text{Nb}} = 17 \mu\Omega \text{ cm}$, we estimate $\ell_{e,\text{Nb}} \approx 2.3$ nm and $\xi_{\text{Nb}} \approx 5.8$ nm, respectively, using Eqs. (A1), (A9), and (A10). For Pd_{0.81}Ni_{0.19}, we assume that the mean free path is thickness limited, and using an average value of $\ell_{e,\text{PdNi}} \approx 3.5$ nm and the measured $\rho_{\text{PdNi}} = 64 \mu\Omega \text{ cm}$, we find the coherence length in the ferromagnet $\xi_F^* = 6.2$ nm. The characteristic length ξ_F^* sets the diffusion length scale for Cooper pairs as in a normal metal, without reference to the exchange energy. It should not be confused with $\xi_F = \sqrt{(\hbar D_F)/E_{\text{ex}}}$, which in the dirty limit is both the superconducting correlation decay length (and therefore often called the coherence length) and the superconducting correlation oscillation length. In fitting, we put

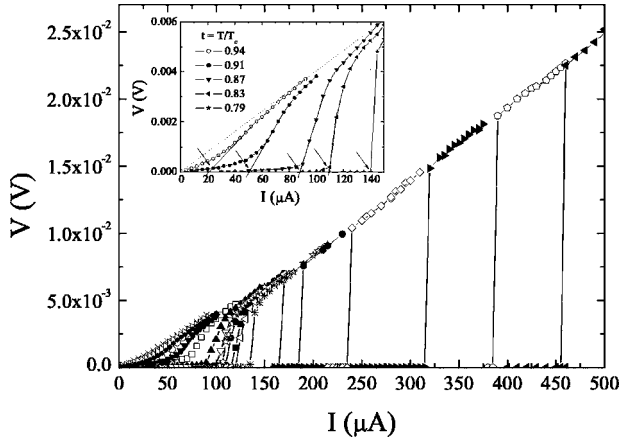


FIG. 5. $V(I)$ characteristics in the reduced temperature range $t = 0.70-1$ for a Nb/Pd_{0.81}Ni_{0.19} bilayer with $d_{\text{PdNi}} = 6.4$ nm. The inset shows the criterion used for J_{dp} close to T_c from the steepest slope of the curves, with the arrows showing the determined values for J_{dp} .

less weight on the data points for very low d_F , below 1.5 nm, because ℓ_{PdNi} becomes considerably lower than the average value. This could have been redressed by making ℓ thickness dependent, but this does not lead to different insights. A good fit for $T_c(d_F)$ is obtained for $E_{\text{ex}} = 230$ K and $\gamma_b = 0.13$, shown as a solid line in Fig. 4. To demonstrate the sensitivity to γ_b , curves for different values of this parameter are also displayed, allowing us to estimate an error bar of $\gamma_b = 0.13 \pm 0.02$. In a similar way, it is possible to evaluate an error bar on the exchange energy value (see inset of Fig. 4), yielding $E_{\text{ex}} = 230 \pm 20$ K ($= 20 \pm 2$ meV). The same parameters were used to evaluate $T_c(d_S)$ (the S series), except that the intrinsic critical temperature dependence of the single Nb films was used for T_{cs} , with 9.2 K as limiting value for thick films. The computed curve is given as a solid line in Fig. 3 and shows very good agreement with the experimental data.

From the value of $E_{\text{ex}} = 230$ K, we can extract $\xi_F = 2.8$ nm. This yields the important value of the oscillation wavelength $\lambda_F = 2\pi\xi_F = 17.6$ nm. It is also possible to estimate ξ_F directly from the position of the minimum in the $T_c(d_F)$ curve, at $d_{\text{PdNi}}^{\text{min}} \approx 3.4$ nm, since d^{min} can be phenomenologically related to ξ_F by $\xi_F \approx 2d^{\text{min}}/0.7\pi = 3.1$ nm,²⁶ in good agreement with the value from E_{ex} . It is of interest to compare these numbers with those for the alloy Pd_{1-x}Ni_x, with $x = 0.14$. In that case, we found $E_{\text{ex}} = 150$ K and $\gamma_b = 0.60$. The first value reflects the smaller magnetic moment in the alloy with $x = 0.14$. The second shows that the interface transparency of the present set of bilayers is significantly higher than in the previous case, which has to do with the fact that these samples were prepared in a different deposition system.

V. DEPAIRING CURRENTS

A. Temperature dependence of J_{dp}

Next we turn to the measurements of the depairing current density J_{dp} , also for the F series. Figure 5 shows the $V(I)$

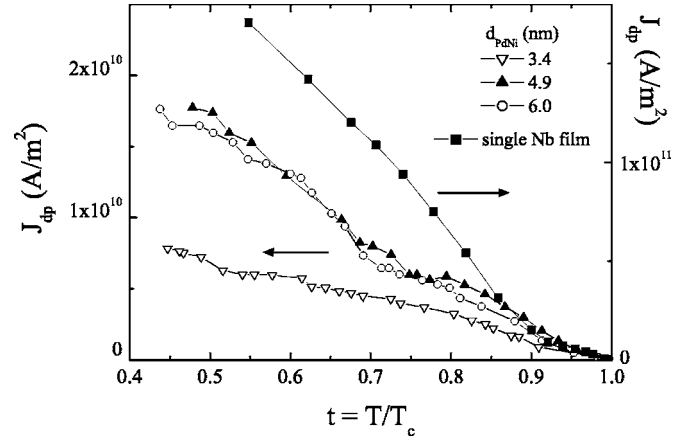


FIG. 6. Dependence of the depairing current density $J_{dp}(t)$ on the reduced temperature t , for a single Nb film (right-hand scale) and for some Nb/Pd_{0.81}Ni_{0.19} bilayers with different d_{PdNi} (left-hand scale). Note the scale difference of almost an order of magnitude.

transitions in the reduced temperature range $t = 0.70-1$ for the Nb/Pd_{0.81}Ni_{0.19} bilayer with $d_{\text{PdNi}} = 6.4$ nm. For all measured bilayers, the curves close to T_c are broader, while the transition to the normal state occurs with a sharp jump as the temperature is lowered. In the first case, the depairing current was defined by extrapolating the steepest slope in $V(I)$ down to $V = 0$, as shown in the inset of Fig. 5. At lower temperatures, J_{dp} was chosen as the value immediately before the transition. From these measurements, it is possible to derive the temperature dependence of the depairing current density, $J_{dp}(T)$, which is shown in Fig. 6 for a few samples. The first observation is that the low-temperature value of J_{dp} strongly decreases in the presence of the PdNi layer, becoming almost an order of magnitude smaller than the value for the single Nb film already around $d_F \approx 2$ nm. The second observation is that all data show an upward curvature with decreasing temperature. This is not unexpected. In earlier work on the system Nb/Fe,¹⁶ we found that, in the Ginzburg-Landau (GL) regime close to T_c ,²⁷ J_{dp} can be described as function of reduced temperature $t = T/T_c$ by the well-known expression

$$J_{dp}^{\text{GL}}(t) = J_{dp}^{\text{GL}}(0)(1-t)^{3/2}, \quad (1)$$

also in the case that the order parameter is not constant over the thickness of the superconducting film. As a first step in the analysis, following Eq. (1), we fit the linear behavior of $J_{dp}^{2/3}$ close to T_c and extrapolate this to $t = 0$ in order to extract $J_{dp}^{\text{GL}}(0)$ (called J_{dp}^0 for short) and to obtain the normalized temperature dependence $J_{dp}(t)/J_{dp}^0$ for all samples. The normalized behavior allows comparison between samples, as well as comparison to the universal form given by the theory of KL,¹⁸ as shown in Fig. 7. The first important observation made from Fig. 7 is that all samples show KL behavior at least down to $t = 0.75$. Moreover, there is no appreciable deviation to values below the KL behavior for any of the measured samples, except possibly for the one with $d_F = 3.4$ nm. Such deviations would be suggestive of heating effects,²² and we conclude that these are mainly absent. The second obser-

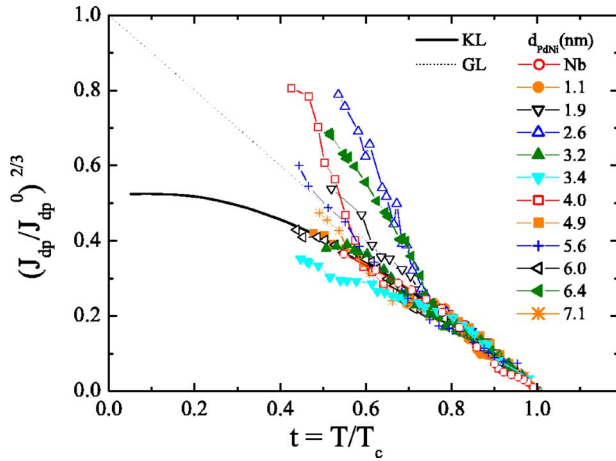


FIG. 7. (Color online) Dependence of the depairing current density J_{dp} , normalized to the extrapolated value J_{dp}^0 , on the reduced temperature t in Nb/Pd_{0.81}Ni_{0.19} bilayers with different d_{PdNi} as indicated. The solid and dotted lines represent the results of the KL and GL theories, respectively.

vation is that a number of samples show clear *positive* deviations from KL behavior.

In order to discuss this further, we first plot the values of T_c and J_{dp}^0 as function of d_F in Fig. 8. Both dependencies look quite similar, with J_{dp}^0 falling off about as quickly as T_c and saturating around $d_F=6$ nm. Also, it is suggestive to think that J_{dp}^0 shows a minimum around $d_F=4$ nm, slightly higher than the minimum in T_c . If the saturation value is taken at 6×10^{10} A/m², the minimum is roughly a factor of 2 lower, and therefore even quite deep in comparison with the minimum in T_c . Unfortunately, the scatter in the data points is also larger, and the data preclude a firm conclusion with respect to the minimum. The origin of this scatter is not fully clear. Thickness variations over the length of the strip are unlikely, given that Rutherford-backscattering spectroscopy and x-ray data show very well-defined values, and at the moment we believe that an unrecognized parameter in the microstructuring process is responsible. The first conclusion is that in the Ginzburg-Landau regime J_{dp} measures the same physics as T_c (which might be expected), and possibly even

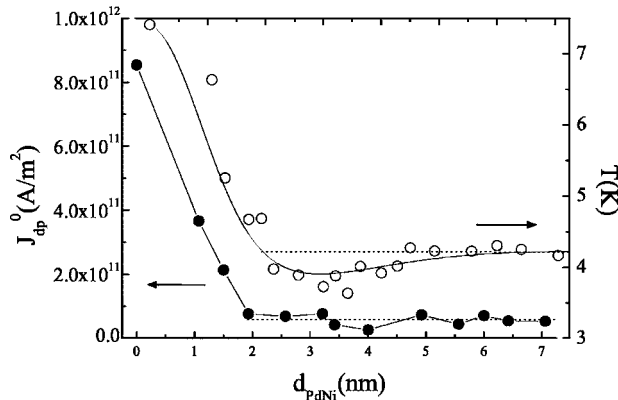


FIG. 8. $T_c(d_{PdNi})$ dependence (\circ) compared to $J_{dp}^0(d_{PdNi})$ behavior (\bullet). The line in $T_c(d_{PdNi})$ is the result of the theoretical fit. The horizontal dotted lines and the thick line are guides for the eyes.

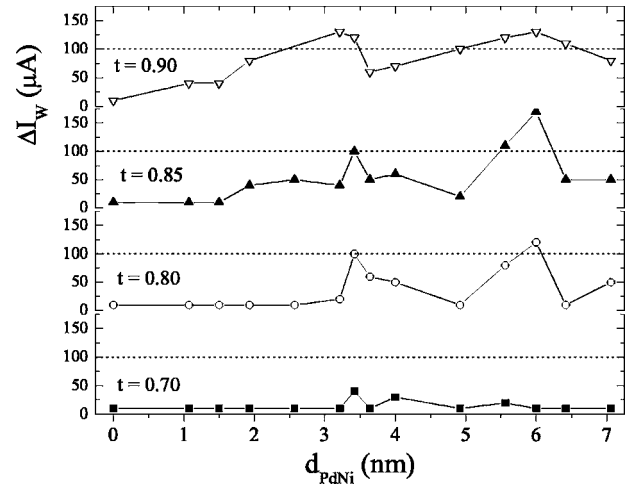


FIG. 9. Dependence of the critical current width ΔI_w of the transition to the normal state (see text for definition) as a function of the Pd_{0.81}Ni_{0.19} thickness d_{PdNi} at different reduced temperatures t . The dotted lines at 100 μ A are guides for the eyes.

more sensitively, but that sample preparation as yet proves an obstacle to gain full benefits.

At lower temperatures, the behavior changes. Our interpretation of the positive deviations of J_{dp} from KL curve is that below a reduced temperature of about $t=0.75$, the inhomogeneous state starts to break up. The high current density apparently allows a relaxation of the order parameter at the S/F interface so that more current can be accommodated in the S layer. The relaxation is far from complete, however, since the values for J_{dp} are still much below the single film values. This effect has not been observed before nor has theoretical work in this regime yet been performed. Looking more closely at Fig. 7, we also observe, however, that positive deviations do not occur for all samples. Specifically, the samples with $d_F=3.2, 3.4, 4.9$, and 6.0 nm stay on the KL curve, which suggests that around the minimum in T_c , when the oscillatory state has set in, the superconducting state becomes more stable.

B. Transition width of the superconducting state to the normal state

At low temperatures, the $V(I)$ characteristics show a sharp jump to the normal state, while close to T_c , this transition is broader, as already mentioned. We investigated for all samples the evolution of the transition width ΔI_w , which was defined as the difference between the current at the onset of a voltage and the current at which Ohmic behavior is recovered. Since in all the measurements a current step of $I_{step}=10$ μ A was used, this is also the smallest value for ΔI_w . Values for ΔI_w are given for different reduced temperatures in Fig. 9. Around $t=0.9$, all samples show some broadening, which generally decreases with decreasing temperature and becomes basically absent around $t=0.7$. Incidentally, this implies that the positive deviations from the KL curve, discussed above, are far outside the width of the transition. Above $t=0.7$, some structure seems to be present in ΔI_w as a function of d_F . Looking more closely, we find that for

$d_F < 3$ nm, the width simply decreases with decreasing t , but that the decrease is slower above this value, and that ΔI_w actually slightly increases at 6 nm. The one anomaly in this data set is the sample at 4.92 nm. Disregarding that for the moment, it is suggestive to assume that the increased width is due to the oscillatory state which sets in above 3 nm and, more specifically, to the node in the order parameter which is present in the oscillatory state, with the largest effect around $\lambda_F/2$. A very similar observation was made on a set of bilayer samples of Nb/Pd_{0.89}Ni_{0.11}, where depairing currents were measured,²⁸ and the transition width peaked around $\lambda_F/2$.

At the moment, a rigorous explanation for these observations is not available. What we can remark is that the state with a node in the order parameter may well be sensitive to experiments involving a supercurrent. We also want to draw attention to a recent theoretical prediction, namely, that in S/F bilayers spontaneous supercurrents may appear *along* the interface for certain thicknesses of the F layer in the π regime.²⁹ In Ref. 29, a two-dimensional (2D) model is analyzed. It is found that Andreev bound states can pile up around zero energy when the superconducting order parameter changes its sign at the F/I interface (I is the vacuum). The resulting state is unstable against the occurrence of spontaneous currents in the plane of the S/F interface. The currents flow in opposite directions in the S and F layers, the total current of the system is zero, and the state should be viewed as a 2D LOFF state. The $\Delta I_w(d_{\text{PdNi}})$ data offer some connection to such a state in the sense that the spontaneous currents and the transport currents both flow along the interface, and therefore may interfere with each other. The broadening might be the result of fluctuations in the S/F interface transparency or the F layer thickness. At the moment, the connection is still tenuous. The calculations were for the clean limit and at $T=0$, and actual numbers for the thickness where the effect occurs may depend on the interface transparency. A more complete explanation will need more data as well as further development of the theory.

VI. SUMMARY

In this study, we have investigated the behavior of the superconducting order parameter in Nb/Pd_{0.81}Ni_{0.19} bilayers by two different methods. The first is the variation of T_c with the thickness of the ferromagnetic layer d_F . These results show the expected behavior with a shallow minimum near $d_F=3$ nm. These data can be quite satisfactorily described by proximity effect theory, with a value for $E_{ex}=230$ K, implying an oscillation wavelength in Pd_{0.81}Ni_{0.19} layer $\lambda_F=17.6$ nm. Both are reasonable numbers for this weakly ferromagnetic alloy. Moreover, we find a quite high interface transparency ($\gamma_b=0.13$) which emphasizes once more the suitability of the Nb/PdNi system for these studies. The second method is the measurement of the depairing current J_{dp} . From this we have drawn several conclusions. In the Ginzburg-Landau regime close to T_c , $J_{dp}(t)$ is found to be proportional to $(1-t)^{3/2}$, similar to single thin superconducting films. As a function of d_F , the extrapolated values $J_{dp}(0)$ show a behavior very similar to $T_c(d_F)$, with a minimum at

the slightly higher value of $d_F=4$ nm. The minimum is also less shallow than in the case of $T_c(d_F)$, but this is somewhat masked by a larger sample-to-sample variation. Going to lower temperatures, $J_{dp}(t)$ still follows the theoretical (Kupriyanov-Lukichev) behavior of single films, but at temperatures below $t=0.75$, we start to observe deviations to larger-than-expected current densities. We interpret this as a relaxation of the superconducting order parameter at the S side of the S/F interface, so that more current can flow through the sample. We also find, however, that this tendency to higher current densities is less for larger values of d_F , in the regime where the oscillatory order parameter occurs, which indicates a higher stability for this state. Finally, we found that the width of the current-induced transition to the normal state behaves in a nonintuitive fashion. For small d_F , the width goes down with decreasing temperature, but around $d_F=6$ nm, which is well into the oscillatory state, the value remains high for a larger range of temperatures (although still close to the GL regime). We have not found a clear explanation for the latter observation, and we can only speculate that, around this particular thickness, the appearance of spontaneous supercurrents at the Nb/PdNi interface may play a role, which, if confirmed, would point to a 2D LOFF state.

ACKNOWLEDGMENTS

We thank R. Hendrikx and M. Hesselberth for supportive x-ray and Rutherford-backscattering measurements. This work is part of the research program of the “Stichting voor Fundamenteel Onderzoek der Materie (FOM),” which is financially supported by the “Nederlandse Organisatie voor Wetenschappelijk Onderzoek (NWO).”

APPENDIX: PROXIMITY EFFECT CALCULATIONS

Here we briefly reiterate the main formulas used for fitting the data of $T_c(d_F)$ and $T_c(d_S)$ (see Sec. IV) in the so-called single-mode approximation. For details, we refer to Refs. 17 and 26. We first define the following symbols:

$$\xi_S = \sqrt{\frac{\hbar D_S}{2\pi k_B T_{cS}}}, \quad \xi_F^* = \sqrt{\frac{\hbar D_F}{2\pi k_B T_{cS}}}, \quad (\text{A1})$$

$$\gamma = \frac{\rho_S \xi_S}{\rho_F \xi_F^*}, \quad \gamma_b = \frac{R_B \mathcal{A}}{\rho_F \xi_F^*}. \quad (\text{A2})$$

Here $\rho_{S,F}$ and $D_{S,F}$ are the low-temperature resistivities and the diffusion coefficients in S and F , respectively, while R_B is the normal-state boundary resistivity and \mathcal{A} is its area. The parameter γ is a measure of the strength of the proximity effect between the S and F metals, while γ_b describes the effect of the interface transparency \mathcal{T} according to

$$\gamma_b = \frac{2 \ell_F}{3 \xi_F^*} \frac{1 - \mathcal{T}}{\mathcal{T}}. \quad (\text{A3})$$

The critical temperature of the bilayer is then determined by the equations

$$\ln\left(\frac{T_{cS}}{T_c}\right) = \Psi\left(\frac{1}{2} + \frac{\Omega^2 T_{cS}}{2 T_c}\right) - \Psi\left(\frac{1}{2}\right), \quad (\text{A4})$$

$$\Omega \tan\left(\Omega \frac{d_S}{\xi_S}\right) = W(\omega_n), \quad \omega_n = \pi T_c(2n+1), \quad (\text{A5})$$

with

$$W(\omega_n) = \gamma \frac{A_S(\gamma_b + \text{Re } B_F) + \gamma}{A_S|\gamma_b + B_F|^2 + \gamma(\gamma_b + \text{Re } B_F)}, \quad (\text{A6})$$

$$B_F = [k_F \xi_F^* \tanh(k_F d_F)]^{-1}, \quad k_F = \frac{1}{\xi_F^*} \sqrt{\frac{|\omega_n| + iE_{ex} \text{sgn } \omega_n}{\pi k_B T_{cS}}}, \quad (\text{A7})$$

$$A_S = k_S \xi_S \tanh(k_S d_S), \quad k_S = \frac{1}{\xi_S} \sqrt{\frac{\omega_n}{\pi k_B T_{cS}}}, \quad (\text{A8})$$

where $W(\omega_n)$ is considered ω_n independent by taking only the first value of $\omega = \omega_0 = \pi T_c$. Here $\Psi(x)$ is the digamma

function and T_{cS} is the critical temperature of the single S layer. Several microscopic parameters can be derived from the experimentally determined resistivities. The coherence lengths $\xi_{S,F}$ can be determined through Eq. (A1), where $D_{S,F}$ is related to the low-temperature resistivity $\rho_{S,F}$ through the electronic mean free path $\ell_{S,F}$ by

$$D_X = \frac{v_X \ell_X}{3}, \quad X = S, F, \quad (\text{A9})$$

in which

$$\ell_X = \frac{1}{v_X \gamma_X \rho_X} \left(\frac{\pi k_B}{e} \right)^2, \quad X = S, F, \quad (\text{A10})$$

where $\gamma_{S,F}$ and $v_{S,F}$ are the electronic specific heat coefficient and the Fermi velocity of the S, F material, respectively. For Nb, $\gamma_{\text{Nb}} \approx 7 \times 10^{-4} \text{ J/K}^2 \text{ cm}^3$ (Ref. 30) and $v_S \equiv v_{\text{Nb}} = 2.73 \times 10^7 \text{ cm/s}$.³¹ For PdNi, we use the Pd Fermi velocity $v_F \equiv v_{\text{Pd}} = 2.00 \times 10^7 \text{ cm/s}$.³²

*Present address: Dipartimento di Fisica “E.R. Caianiello” and Laboratorio Regionale SuperMat INFM-Salerno, Università degli Studi di Salerno, Baronissi (Sa) I-84081, Italy.

†Present address: Institute of Solid State Physics, Russian Academy of Sciences, Chernogolovka 142432, Russia.

¹A. I. Buzdin, Rev. Mod. Phys. **77**, 935 (2005).

²E. A. Demler, G. B. Arnold, and M. R. Beasley, Phys. Rev. B **55**, 15174 (1997).

³A. I. Larkin and Yu. N. Ovchinnikov, Sov. Phys. JETP **20**, 762 (1965).

⁴P. Fulde and R. A. Ferrell, Phys. Rev. **135**, A550 (1964).

⁵I. A. Garifullin, J. Magn. Magn. Mater. **240**, 571 (2002).

⁶T. Kontos, M. Aprili, J. Lesueur, F. Genet, B. Stephanidis, and R. Boursier, Phys. Rev. Lett. **89**, 137007 (2002).

⁷A. I. Buzdin and M. Y. Kupriyanov, JETP Lett. **53**, 321 (1991).

⁸V. V. Ryazanov, V. A. Oboznov, A. Yu. Rusanov, A. V. Veretennikov, A. A. Golubov, and J. Aarts, Phys. Rev. Lett. **86**, 2427 (2001).

⁹T. Kontos, M. Aprili, J. Lesueur, and X. Grison, Phys. Rev. Lett. **86**, 304 (2001).

¹⁰A. I. Buzdin, A. V. Vedyayev, and N. V. Ryzhanova, Europhys. Lett. **48**, 686 (1999).

¹¹L. R. Tagirov, Phys. Rev. Lett. **83**, 2058 (1999).

¹²I. Baladié, A. Buzdin, N. Ryzhanova, and A. Vedyayev, Phys. Rev. B **63**, 054518 (2001).

¹³J. Y. Gu, C.-Y. You, J. S. Jiang, J. Pearson, Ya. B. Bazaliy, and S. D. Bader, Phys. Rev. Lett. **89**, 267001 (2002).

¹⁴A. Potenza and C. H. Marrows, Phys. Rev. B **71**, 180503(R) (2005).

¹⁵I. C. Moraru, W. P. Pratt, Jr., and N. O. Birge, Phys. Rev. Lett. **96**, 037004 (2006).

¹⁶J. M. E. Geers, M. B. S. Hesselberth, J. Aarts, and A. A. Golubov, Phys. Rev. B **64**, 094506 (2001).

¹⁷Ya. V. Fominov, N. M. Chitchev, and A. A. Golubov, Phys.

Rev. B **66**, 014507 (2002).

¹⁸M. Yu. Kupriyanov and V. F. Lukichev, Fiz. Nizk. Temp. **6**, 445 (1980) [Sov. J. Low Temp. Phys. **6**, 210 (1980)].

¹⁹C. Cirillo, C. Bell, and J. Aarts (unpublished).

²⁰W. J. Skocpol, Phys. Rev. B **14**, 1045 (1976).

²¹J. W. Bremer and V. L. Newhouse, Phys. Rev. **116**, 309 (1959).

²²A. Yu. Rusanov, M. B. S. Hesselberth, and J. Aarts, Phys. Rev. B **70**, 024510 (2004).

²³J. Beille, Ph. D. thesis, Université Joseph Fourier, Grenoble, 1975.

²⁴M. Yamada and S. Tanda, Physica B **281-282**, 384 (2000).

²⁵S. I. Park and T. H. Geballe, Physica B & C **135**, 108 (1985).

²⁶C. Cirillo, S. L. Prischepa, M. Salvato, C. Attanasio, M. Hesselberth, and J. Aarts, Phys. Rev. B **72**, 144511 (2005).

²⁷V. L. Ginzburg and L. D. Landau, Zh. Eksp. Teor. Fiz. **20**, 1064 (1950).

²⁸The increased transition width in Nb/Pd_{0.89}Ni_{0.11} is unpublished. Depairing current data can be found in A. Yu. Rusanov, J. Aarts, M. Aprili, in the *Proceedings of the NATO Advanced Research Workshop on Nanoscale Devices—Fundamentals and Applications, Kishinev, Moldova, 18–22 September 2004*, NATO Science Series II: Mathematics, Physics and Chemistry Vol. 233, edited by R. Gross, A. Sidorenko, and L. Tagirov (Springer, New York, 2006), p. 127.

²⁹M. Krawiec, B. L. Györfy, and J. F. Annett, Phys. Rev. B **66**, 172505 (2002); Eur. Phys. J. B **32**, 163 (2003); Physica C **387**, 7 (2003); Phys. Rev. B **70**, 134519 (2004).

³⁰*Handbook of Chemistry and Physics*, edited by R. C. Weast (CRC, Cleveland, OH, 1972).

³¹H. R. Kerchner, D. K. Christen, and S. T. Sekula, Phys. Rev. B **24**, 1200 (1981).

³²L. Dumoulin, P. Nedellec, and P. M. Chaikin, Phys. Rev. Lett. **47**, 208 (1981).